Published in final edited form as:
J Control Release. 2006 August 28; 114(2): 130–142. doi:10.1016/j.jconrel.2006.06.005.

Manipulation of hydrogel assembly and growth factor delivery via the use of peptide-polysaccharide interactions

Le Zhang[a], **Eric M. Furst**[b], and **Kristi L. Kiick**[a,*]

a*Department of Materials Science and Engineering, University of Delaware, Newark, DE 19716, United States*

b*Department of Chemical Engineering, University of Delaware, Newark, DE 19716, United States*

Abstract

The design of materials in which assembly, mechanical response, and biological properties are controlled by protein-polysaccharide interactions could provide materials that mimic the biological environment and find use in the delivery of growth factors. In the investigations reported here, a heparin-binding, coiled-coil peptide, $PF4_{ZIP}$, was employed to mediate the assembly of heparinized polymers. The heparin-binding affinity of this peptide was compared with that of other heparin-binding peptides (HBP) via heparin-sepharose chromatography and surface plasmon resonance (SPR) experiments. Results from these experiments indicate that $PF4_{ZIP}$ demonstrates a higher heparin-binding affinity and heparin association rate when compared to the heparin-binding domains of antithrombin III (ATIII) and heparin-interacting protein (HIP). Viscoelastic hydrogels were formed upon the association of $PF4_{ZIP}$-functionalized star poly(ethylene glycol) (PEG-$PF4_{ZIP}$) with low-molecular-weight heparin-functionalized star PEG (PEG-LMWH). The viscoelastic properties of the hydrogels can be altered via variations in the ratio of LMWH to $PF4_{ZIP}$. bFGF release from these gels have also been investigated. Comparison of the bFGF release profiles with the hydrogel erosion profiles indicates that bFGF delivery from this class of hydrogels is mainly an erosion-controlled process and the rates of bFGF release can be modulated via choice of HBP or via variations in the mechanical properties of the hydrogels. Manipulation of hydrogel physical properties and erosion profiles will provide novel materials for controlled growth factor delivery and other biomedical applications.

Keywords

Coiled-coil peptide; Polysaccharide; Hydrogel assembly; Mechanical properties; Basic fibroblast growth factor

1. Introduction

Polysaccharides and glycoproteins are widely spread on the surface of cells and in the extracellular matrix (ECM) *in vivo*, and accordingly, protein-polysaccharide recognition regulates a myriad of physiological and pathological processes, such as cell proliferation, inflammation and internalization of extracellular proteins. In particular, glycosaminoglycans have been demonstrated to mediate a wide range of biological activities such as cell adhesion, cell mobility, cell proliferation and tissue morphogenesis via binding to various cell regulatory proteins such as the chemokines, growth factors, enzymes, enzyme inhibitors, and extracellular matrix proteins [1-3]. The well studied glycosaminoglycan, heparin, is a linear, unbranched,

*Corresponding author. *E-mail address:* kiik@UDel.edu (K.L. Kiick)..

highly sulfated polysaccharide chain [4,5], and it is well accepted that the electrostatic interactions between the sulfates of the glycosaminoglycan and basic residues of a protein play an important role in binding [6]. In particular, the spatial orientation of the basic residues is a major determinant of heparin-binding affinity [7], and variations in the pattern of the sulfation of the heterogeneous heparin therefore permit binding between heparin and a wide range of binding partners [8,9]. Accordingly, heparin has been incorporated into covalent hydrogel delivery systems because of this ability to bind a diverse set of proteins. In addition, we and others have demonstrated that the interactions between heparin and specific HBPs can also mediate the assembly of noncovalently associated hydrogel networks [10-12].

Because hydrogels can mimic the high water content and mechanical properties of natural tissues, [13] they are prime candidates as carriers of bioactive agents, in bioadhesive systems, or as biorecognizable materials. Given that PEG is highly hydrophilic and generally nonadhesive to proteins or cells, it has found widespread use as a drug carrier [14], and many PEG hydrogels have been produced from aqueous solutions containing linear or branched PEG macromolecules via chemical crosslinking [15-18]. In addition to hydrogels formed via radical crosslinking reactions, PEG hydrogels have been formed, for example, via Michael-type addition reactions upon mixing with thiol-bearing compounds [19,20] or via the reaction between amino-terminated poly (ethylene glycol) and the herbal iridoid glycoside genipin [21]. In some cases, cell adhesive peptide domains or biodegradable sequences have been introduced into PEG hydrogels to endow them with biological signaling functions [22], including the capacity for growth factor delivery. Accordingly, there have been a variety of covalently crosslinked hydrogel systems developed to deliver growth factors via mechanisms such as diffusion and chemical or enzymatic reaction [23-28].

Noncovalent interactions provide an alternative method for crosslinking, as introduced above, removing the need for toxic chemical crosslinking agents in gel preparation [29]. In addition, noncovalent crosslinking strategies may offer advantages in maintaining protein integrity and bioactivity until delivery. Polymer hydrogels have been formed via specific recognition events such as reversible antibody-antigen interactions [30] and coiled-coil interactions [31-33]. There has been less attention given, however, to the interaction between peptides (particularly coiled-coils) and polysaccharides in hydrogel assembly. Here, we report our continuing efforts toward manipulating both the physical properties of and protein delivery from hydrogels via heparin-peptide interactions. Specifically, hydrogels were assembled via interactions between LMWH and $PF4_{ZIP}$, a coiled-coil heparin-binding peptide modeled after the heparin-binding domain of human platelet factor 4 [34]. Mechanical properties, bFGF release profiles, and hydrogel erosion kinetics have been monitored and compared with the previous hydrogel systems. Manipulation of hydrogel physical properties and erosion profiles will provide novel materials for a controlled growth factor delivery and other biomedical applications.

2. Materials and methods

2.1. Materials

Hydroxy-terminated four-arm PEG (M_n=10,300; M_w=11,300 g/mol) and thiol terminated, four-arm PEGs (M_n=10,000; M_w=10,800 g/mol) were obtained from Polymer Source (Dorval, Quebec, Canada). Low molecular weight heparin sodium salt (LMWH) from porcine intestinal mucosa (avg. molecular weight 3000 g/mol) was purchased from Sigma (St. Louis, MO), and heparin from porcine intestinal mucosa (avg. molecular weight 6000 g/mol) was purchased from Celsus Lab., Inc. (Cincinnati, OH). Deionized water (18 MΩ) was used in all experiments (Barnstead NANOpure Diamond Ultrapure water Systems, Barnstead Inc, Dubuque, IO). Amino acids, rink amide MBHA (4-methylbenzhydrylamine) resin, and HBTU were obtained from Novabiochem Corp. (San Diego, CA). DMF and acetonitrile (HPLC grade) were purchased from Fisher Scientific (Fairlawn, NJ). General chemicals were all obtained from

Sigma-Aldrich unless otherwise specified. Triethylamine (TEA) was distilled from CaH_2. All other reagents were used as received.

2.2. Methods

2.2.1. Synthesis of PEG-LMWH conjugates—*Synthesis of PEG-LMWH.* The synthesis of the PEG-LMWH conjugate exploited in hydrogel assembly was conducted via Michael-type addition reactions between maleimide functionalized heparin and thiol-terminated four-arm star PEG, as previously reported [10]. The degree of LMWH functionalization in PEG-LMWH was determined to be 81% via ^{1}H NMR spectroscopy. *Synthesis of PEG-LMWH-Alexa Fluor 350.* PEG-LMWH-Alexa Fluor 350 was synthesized to facilitate tracking of the eroded PEG-LMWH via fluorimetry. The synthesis protocol was described in detail previously [35].

2.2.2. Synthesis of PEG-PF4$_{ZIP}$ conjugates—PF4$_{ZIP}$Synthesis. PF4$_{ZIP}$ was prepared on Rink Amide MBHA resin via solid phase peptide synthesis with Fmoc-protection using a PTI PS3 peptide synthesizer (Protein Technologies Inc, Tucson, AZ). The PF4$_{ZIP}$ sequence CGGRMKQLEDKVKKLLKKNYHLENEVARLKKLVG is based on a GCN4 coiled-coil and mimics the heparin-binding domain of human platelet factor 4 [34]. The previously reported heparin-binding peptides, ATIII and HIP peptides, from antithrombin III (ATIII) and heparin interacting protein (HIP), included here for comparison, were synthesized according to similar protocols [10,11]. The crude peptides were purified via preparative-scale HPLC (Waters Delta 600, Waters Corporation, Milford, MA) equipped with a Waters Symmetry 300 C18 column (5 μm particle size, 19×150 mm). Two HPLC solvents - solvent A (water/0.1% TFA) and solvent B (acetonitrile/0.1% TFA) - were used in programmed gradients. Peptides isolated as single fractions via HPLC were characterized via MALDI and ESI mass spectrometry. The mass of the purified PF4$_{ZIP}$ was confirmed via ESI mass spectrometry, m/z=992.5 [$(M+4H)^{4+}$, calc'd 992.0] and m/z=1322.9 [$(M+3H)^{3+}$, calc'd 1322.7]. *Synthesis of PEG-PF4$_{ZIP}$.* The synthesis of the PEG-PF4$_{ZIP}$ conjugate utilized in hydrogel assembly was conducted via Michael addition reactions between vinyl sulfone-terminated four-arm PEG and cysteine-terminated PF4$_{ZIP}$ peptide, using a similar method applied previously for the synthesis of other PEG-HBP conjugates [10].

2.2.3. Assembly of PEG-LMWH/PEG-PF4$_{ZIP}$hydrogels—The PEG-LMWH/PEG-PF4$_{ZIP}$ hydrogels were formed by the interaction between LMWH and PF4$_{ZIP}$. 5 wt.% solutions of the PEG-PF4$_{ZIP}$ in PBS were added directly to 2.5 wt.% solutions of the PEG-LMWH in PBS, to afford hydrogel networks at a final composition of 2.5 wt.% total polymer. The solutions were mixed in ligand mole ratios of 9:0.5, 8:1, and 7.5:2.5 (LMWH:PF4$_{ZIP}$ dimer). After mixing, the hydrogels were stored at 4 °C. The stored hydrogels were equilibrated to room temperature prior to rheological characterization (typically several minutes).

2.2.4. ^{1}H NMR spectroscopy—^{1}H NMR spectra were acquired on a Bruker DRX-400 NMR spectrometer (Bruker Daltonics, Billerica, MA). DMSO-*d6* or deuterium oxide was used as the NMR solvent and TMS or DSS as references, respectively. All the spectra were acquired under standard quantitative conditions.

2.2.5. Matrix assisted laser desorption ionization-time of flight (MALDI-TOF) and electrospray mass spectrometry—MALDI-TOF mass spectra were acquired on a Bruker Biflex III mass spectrometer (Bruker Daltonics, Billerica, MA). Reflection mode and delayed extraction were used to acquire the spectra. All MALDI samples were dissolved in 50% acetonitrile in 0.3% TFA with the matrix α-cyano-4-hydroxycinnamic acid. A Finnigan LCQ electrospray ion trap mass spectrometer (Thermo Electron Corp, San Jose, CA) was used to obtain the electrospray spectra. Methanol was used as the solvent in all electrospray experiments.

2.2.6. Circular dichroic spectroscopy (CD)—CD spectra were measured at 5 °C to 75 °C on a Jasco J-810 spectropolarimeter (Jasco Inc, Easton, MD) equipped with a Jasco PTC-424S temperature controller. Samples were equilibrated at the desired temperature for 30 min prior to data collection; equilibration was indicated by the absence of further changes in the CD signal at longer equilibration times. All CD spectra were taken in a 1 mm path length quartz cuvette, at wavelengths from 200 to 250 nm. Data points were recorded at every nanometer with a 4.0 s response time. The concentrations of peptide samples were determined via amino acid analysis for calculation of mean residue ellipticities.

2.2.7. Heparin affinity measurements—*Affinity Liquid Chromatography*. Heparin-sepharose affinity liquid chromatography was performed on an ÄKTA Explorer FPLC equipped with a HiTrap Heparin HP column (5 ml, ~10 mg heparin/ml gel, Amersham Biosciences Corp, Piscataway, NJ), as previously described [10]. *Surface Plasmon Resonance (SPR)*. SPR sensorgrams were recorded on a BiaCore 3000 instrument (Biacore Inc, Piscataway, NJ), employing a high-capacity LMWH surface created on a commercially available streptavidin-coated chip via treatment with biotinylated LMWH, as previously described [11].

2.2.8. Bulk rheology experiments—Bulk rheology experiments of the PEG-LMWH/PEG-$PF4_{ZIP}$ hydrogels were conducted at 25 or 37 °C on a stress-controlled rheometer (MCR 500, Paar Physica, Anton-Paar, Ashland, VA) with a 25.0 mm diameter parallel plate geometry and a 1 mm gap distance. Sample preparation was as previously reported [10]. Strain sweeps were performed on samples from 0.001% to a maximum strain of 100% to determine the limit of the linear viscoelastic regime (LVE). At a constant strain of 0.1%, chosen from the LVE, frequency sweeps ranging from 0.1 rad/s to 100 rad/s were conducted. Shear recovery experiments were also performed, and prior to these experiments, a baseline oscillation at a constant strain of 0.1% and a constant frequency of 10 rad/s was performed, followed by a high-speed rotation with a 1000 s^{-1} shear rate for 10 s. The recovery was then measured with a time sweep experiment at a constant strain of 0.1% and a constant frequency of 10 rad/s.

2.2.9. Fluorimetry experiments—Fluorimetry experiments to measure the concentration of PEG-LMWH-Alexa Fluor 350 were performed using a FluoroMax-3 spectrofluorometer (Jobin Yvon Inc, Edison, NJ) with a xenon arc lamp illuminater. 45 μL of each sample were loaded into a cuvette and excited at 346 nm, the excitation spectra peak value of Alexa Fluor 350. The emission spectra peak value at 442 nm was recorded. Solutions of PEG-LMWH-Alexa Fluor 350 in PBS, with concentrations from 5.42×10^{-4} wt.% to 4.23×10^{-6} wt.%, were employed for generation of the standard curve. For erosion profile experiments, the PEG-LMWH-Alexa Fluor 350 was premixed with the PEG-LMWH at a weight ratio of 1:158. The fluorescence intensities of the PEG-LMWH-Alexa Fluor 350 in the eroded PEG-LMWH were then measured and permitted calculation of the percentage of PEG-LMWH eroded from the hydrogels in hydrogel erosion experiments.

2.2.10. bFGF release and hydrogel erosion experiments—bFGF release and hydrogel erosion experiments were performed at 4 °C in 24-well polystyrene assay plates (Corning Inc., Corning, NY), blocked with PBS containing 5% BSA and 0.05% Tween 20 (Sigma, St. Louis, MO). The wells were aspirated and washed 4 times with 0.05% Tween 20 in PBS before loading samples. Afterward, 200 μL hydrogel was placed on the bottom of each well and 2.8 mL PBS was added carefully over each gel. 1 mL PBS was taken out of the well at 1, 2, 6 and 24 h and then each following day, followed by replacement with 1 mL fresh PBS. The amount of bFGF in each sample was measured with a bFGF Quantikine kit (R&D Systems, Minneapolis, MN). The hydrogel erosion kinetics were conducted on the same samples used for bFGF release experiments.

3. Results

3.1. Oligomerization of $PF4_{ZIP}$

Our initial studies were aimed at determining the oligomerization properties of the coiled-coil $PF4_{ZIP}$, as such information is relevant to the subsequent use of the $PF4_{ZIP}$ in hydrogel formation. A variety of studies have already been conducted on the thermodynamics and kinetics of unfolding equilibria for the GCN4 coiled-coil. Most results are in agreement that the GCN4 coiled-coil monomer-dimer transition follows a two-state equilibrium [36-39], although there is some evidence that there is more than one folded form [40,41]. Circular dichroic spectroscopy studies were conducted to assess the folding of the $PF4_{ZIP}$ under various conditions. Solutions of $PF4_{ZIP}$ dissolved in PBS were scanned from 250 nm to 200 nm at varying temperatures between 5 °C and 75 °C. The CD spectra of $PF4_{ZIP}$ at a variety of temperatures (Fig. 1)show an isodichroic point at 203 nm, validating the existence of a two-state equilibrium between the coiled-coil and random-coil forms of the peptide. At temperatures below 55 °C, the spectra observed exhibit two minima at 208 nm and 222 nm, demonstrating that $PF4_{ZIP}$ exists in the coiled-coil state under conditions of interest for hydrogel applications. As seen by the appearance of a single minimum at 203 nm in the data collected at elevated temperatures, the structure of $PF4_{ZIP}$ reversibly changes to random-coil at elevated temperature. Maximum mean residue ellipticity values at 222 nm (MRE_{222}) were measured to be -30,470 deg cm^2 $dmol^{-1}$ for the $PF4_{ZIP}$ at 15 °C, consistent with reported values ranging from -25,000 to -35,000 deg cm^2 $dmol^{-1}$ for various GCN4-mimic peptides in PBS at 15 °C [42,43].

The conformation of $PF4_{ZIP}$ at various concentrations was also monitored via CD, as shown in Fig. 2(a). At all measured concentrations, the spectra observed exhibit two minima at 208 nm and 222 nm, demonstrating the helical character of $PF4_{ZIP}$ under these conditions. The measured MRE_{222} for a solution of 56 μM $PF4_{ZIP}$ in PBS is -24,580 deg cm^2 $dmol^{-1}$, which is consistent with the value reported for 40-60 μM $PF4_{ZIP}$ in 3 mM sodium citrate buffer (-27,000 deg cm^2 $dmol^{-1}$) [34]. As shown in the Appendix, the difference between the measured ellipticity and the ellipticity of the unfolded monomer, $\Delta\theta$, is related to concentration and can be fit to determine the K_d of dimerization. The best fit of the concentration dependence of $\Delta\theta$, according to Eq. (A4), is shown in Fig. 2(b). The calculated equilibrium constant of unfolding, K_d, is 3.48±0.03 μM. Solutions of $PF4_{ZIP}$ attached to the star PEG were also studied via CD, to ensure that conjugation to PEG did not significantly alter the association of the $PF4_{ZIP}$ coiled-coils. As shown in Fig. A1(a), the spectra of PEG-$PF4_{ZIP}$ are essentially identical to the spectra obtained for the isolated $PF4_{ZIP}$. Slight differences in MRE values likely arise from uncertainties in the precise peptide concentrations for the PEG-$PF4_{ZIP}$ samples. The K_d value derived from the best fit of the concentration dependence of $\Delta\theta$ (Fig. A1(b)) for PEG-$PF4_{ZIP}$ is 0.93 μM. The $PF4_{ZIP}$ concentrations during NMR characterization and hydrogel formation and characterization are always much greater than these measured K_d values (e.g., 200 μM and higher), suggesting that $PF4_{ZIP}$ will exist primarily as a dimer under those conditions.

3.2. Heparin-binding affinity

Our previous investigations of PEG-LMWH/PEG-HBP hydrogels suggested that the viscoelastic properties of the noncovalently assembled hydrogels were consistent with the heparin-binding kinetics of the peptides (from antithrombin III (ATIII) or heparin interacting protein (HIP)) [11]. Heparin-sepharose affinity chromatography and SPR experiments were therefore used to compare the heparin-binding affinity of $PF4_{ZIP}$ with those measured for the previously prepared peptides [11] in order to confirm the potential of $PF4_{ZIP}$ to mediate hydrogel formation. Results of these experiments are summarized in Table 1. For heparin affinity chromatography experiments, $PF4_{ZIP}$ was loaded onto a heparin-sepharose column,

and then eluted with buffer of increasing NaCl concentration. The concentration of NaCl required for peptide elution is used as an indication of the affinity of the peptide for heparin. The elution of the peptides from the heparin-sepharose column required a salt concentration of 962 ± 10 mM for the $PF4_{ZIP}$ peptide. The salt concentration required to elute $PF4_{ZIP}$ (962 ± 10 mM) is higher than that measured for the ATIII peptide (594± 2 mM) and for the HIP peptide (687± 1 mM), indicating that $PF4_{ZIP}$ has higher heparin-binding affinity than the ATIII and HIP peptides and should therefore be competent for hydrogel assembly. These results are consistent with previous reports indicating that similarly high concentrations of NaCl were required to elute ^{125}I-labeled $PF4_{ZIP}$ bound to a heparin-sepharose column in 0.02 M Tris-HCl buffer pH 7.0 containing 0.05 M NaCl [34].

In SPR experiments, the interaction of the peptides with a LMWH-modified SA chip surface was determined under conditions described in the experimental section. Neither nonspecific binding of heparin-binding peptides to SA chips nor chip instability was observed in any of the SPR measurements. In addition, no mass transport limitation or linked reactions were indicated. The binding curves for the interaction of the peptides with the LMWH-modified chip surface are shown in Fig. A3 and analysis of the association and dissociation regions of the binding curves provided association and dissociation rates for comparison to previous studies [10]. The measured association of the $PF4_{ZIP}$ with LMWH proceeds with a rate constant of $2.24\pm0.05\times10^{5}$ $M^{-1}s^{-1}$, while the dissociation proceeds with a rate constant of $2.56\pm0.10\times10^{-3}$ s^{-1}, yielding a K_D of approximately $1.15\pm0.03\times10^{-2}$ μM. Comparison to results from our previous studies indicates that these faster association kinetics, relative to those reported for the ATIII and HIP [11], are the primary cause of the lower measured K_D values for $PF4_{ZIP}$-LMWH binding, and the trend of the equilibrium dissociation constants is consistent with the chromatography results. The more rapid association rate, coupled with the similar dissociation rate, of $PF4_{ZIP}$ versus the other HBPs, points to the successful formation of hydrogels between PEG-$PF4_{ZIP}$ and PEG-LMWH. The measured K_D of the binding between $PF4_{ZIP}$ and LMWH is lower than the measured K_d of dissociation of the coiled-coil obtained from CD experiments, which may suggest that the LMWH-functionalized surface facilitates coiled-coil formation or that the monomeric form of the peptide also exhibits affinity for the LMWH-functionalized surface. Nevertheless, the equilibrium constants of dissociation determined via both methods are substantially lower than the concentrations employed during hydrogel formation experiments (see below).

3.3. Temperature dependence of $PF4_{ZIP}$ binding

The heparin-binding kinetics between LMWH and $PF4_{ZIP}$ were monitored via SPR at several temperatures between 5 °C and 37 °C, to determine potential changes in binding kinetics that might alter hydrogel properties under physiological conditions. Data from these experiments are shown in Table 2. The measured on and off rates fluctuate only slightly throughout the temperature range, suggesting that noncovalently assembled hydrogels based on $PF4_{ZIP}$ and LMWH interactions should exhibit consistent mechanical properties at these temperatures.

3.4. PEG-LMWH/PEG-$PF4_{ZIP}$ hydrogel formation

The composition of the PEG-$PF4_{ZIP}$ was determined from its ^{1}H NMR spectrum, shown in Fig. A2. The functionalization of the star PEG with $PF4_{ZIP}$ dimer in PEG-$PF4_{ZIP}$ is determined to be 59% via NMR (see Appendix), indicating that an average of 2.4 out of four-arms of the star PEG had been functionalized with the $PF4_{ZIP}$ dimer and that therefore PEG-$PF4_{ZIP}$ would meet the functional requirement (f> 2) for crosslinking a hydrogel upon interaction with PEG-LMWH (which showed a functionalization of 81%, as determined via NMR).

Accordingly, solutions of the two polymer conjugates in PBS (2.5 wt.% of the PEG-LMWH and 5 wt.% of the PEG-$PF4_{ZIP}$) were mixed at ligand molar ratios of 9:0.5 and 7.5:2.5 (LMWH:

$PF4_{ZIP}$) to yield the PEG-LMWH/PEG-$PF4_{ZIP}$ hydrogels. The application of such ratios was employed to maximize the excess LMWH available for growth factor binding (see below). Before addition of PEG-$PF4_{ZIP}$, the 2.5 wt.% of the PEG-LMWH was uniform and translucent. In addition, the water-like viscosity of the PEG-$PF4_{ZIP}$ solution indicated that there was no significant crosslinking of the peptide-terminated star polymers via intermolecular coiled-coil formation, although some oligomers of the PEG-$PF4_{ZIP}$ bioconjugates may exist in solution. The formation of self-supporting, opaque gels was immediately apparent upon mixing the two polymer solutions. A schematic of the assembly of the hydrogels is shown in Scheme 1.

3.5. Bulk rheology

The mechanical properties of the PEG-$PF4_{ZIP}$ containing hydrogels were characterized via rheological frequency sweep experiments on bulk samples. The frequency sweep results for PEG-LMWH/PEG-$PF4_{ZIP}$ hydrogels (Fig. 3) show that the storage modulus $G'(\omega)$ is significantly larger than the loss modulus $G''(\omega)$ over all measured frequencies and $G'(\omega)$ exhibits a pronounced plateau extending to frequencies of tens of reciprocal seconds, indicating a viscoelastic gel [44]. The magnitude of $G'(\omega)$ and $G''(\omega)$ also increases as the molar ratio of the peptide component is raised. The average $G'(\omega)$ increases from an average value of 70 Pa for PEG-LMWH to approximately 80 and 180 Pa for hydrogels with molar ratios of LMWH to $PF4_{ZIP}$ of 9:0.5 and 7.5:2.5, respectively. The average $G''(\omega)$ also increases monotonically with higher molar ratio of the peptide component, from less than 10 Pa for PEG-LMWH to more than 30 Pa for hydrogels with molar ratios of LMWH to $PF4_{ZIP}$ of 7.5:2.5. Bulk rheology experiments were also performed on the samples at various gap heights of 1 mm, 0.5 mm, and 0.25 mm. At frequencies from 0.1 to 63 rad/s, identical dynamic moduli at different gap heights were observed, indicating that no significant slipping occurs in that frequency range.

The strengthening effects on storage modulus upon addition of PEG-HBP to PEG-LMWH are presented in Fig. 4 for $G'(\omega=0.1$ rad/s), plotted as a function of the ratio of HBP to LMWH in the samples, with moduli normalized by the initial storage modulus of PEG-LMWH. Data for the hydrogels formed between PEG-LMWH and PEG-HIP or PEG-ATIII are adapted from Ref. [11] and are shown for comparison. The plateau in the modulus with increasing $PF4_{ZIP}$ or HIP concentration may imply that the HBP-binding sites on LMWH have been saturated. Of note is that the increase in the elastic modulus upon addition of PEG-$PF4_{ZIP}$ for the PEG-LMWH/PEG-$PF4_{ZIP}$ hydrogels is lower than that observed with addition of PEG-HBP for the PEG-LMWH/PEG-ATIII or the PEG-LMWH/PEG-HIP hydrogels. Literature reports suggest that at least 4 tetrasaccharides (16 units) are required for efficient heparin-PF4 protein interactions [45], while HIP- and ATIII-binding sites are believed to be similar pentasaccharides in heparin [46]. The LMWH employed in these experiments therefore almost certainly has fewer full-affinity binding sites for the $PF4_{ZIP}$ than for HIP or ATIII, and available binding sites with fewer saccharides may also be of lower affinity. The combination of these effects could lead to the lower storage modulus plateau value and lower slope in Fig. 4 for the PEG-LMWH/PEG-$PF4_{ZIP}$ hydrogels relative to those observed for the PEG-LMWH/PEG-ATIII or the PEG-LMWH/PEG-HIP hydrogels. Nevertheless, the increase in modulus with increasing $PF4_{ZIP}$ concentration confirms the role of $PF4_{ZIP}$ in physically crosslinking the hydrogels.

The rheological properties of the hydrogels were also investigated at physiological temperature. The mechanical properties of the hydrogels with molar ratios of LMWH to $PF4_{ZIP}$ of 9:0.5 and 7.5:2.5 were examined. The frequency sweep data for the hydrogel (LMWH:$PF4_{ZIP}$=9:0.5) are presented in Fig. 5. The moduli at 25 °C or 37 °C are essentially identical, in corroboration of the SPR studies, although the gels at 37 °C exhibit slightly lower loss of moduli at higher frequencies. The materials are therefore also elastic hydrogels at 37 °C. This lack of temperature dependence is also observed in the hydrogel with higher $PF4_{ZIP}$

content, further confirming the temperature insensitivity of both the $PF4_{ZIP}$-LMWH interactions.

Shear recovery data for one of the PEG-LMWH/PEG-$PF4_{ZIP}$ hydrogels are shown in Fig. 6. Both the extent and time-dependence of recovery were determined in these experiments. Due to the heterogeneity of LMWH, the average $G'(\omega)$ (ω=10 rad/s) of the PEG-LMWH-based hydrogels reported in Fig. 6 is significantly lower than that of the hydrogels used in the frequency sweep studies (Fig. 3). Nevertheless, the $G'(\omega)$ of the PEG-LWMWH/PEG-$PF4_{ZIP}$ hydrogels in Fig. 6 show the same increase in elastic moduli with increasing $PF4_{ZIP}$ concentrations, and we show the shear recovery data of these hydrogels here as it represents a limiting case of the slowest measured recovery. Fig. 6 indicates that after the hydrogels are subjected to a steady shear rate of 1000 s^{-1}, they gradually recover their elastic properties, with approximately 30-40% recovery of the elastic modulus after approximately 15 min. Of note is that the identical shear recovery experiments conducted on the hydrogels of greater elastic modulus (Fig. 3), at both 25 °C and 37 °C, indicate over 90% recovery of the initial elastic modulus *immediately* after the application of high shear. The recovery and stability of the PEG-LMWH/PEG-$PF4_{ZIP}$ hydrogels even after subjected to high shear suggests their potential utility in injectable applications.

3.6. Growth factor release and hydrogel erosion

The release of growth factors from these hydrogels in vitro has also been investigated. The utility of the assembled heparinized hydrogels in this kind of application is suggested by the fact that heparin binds bFGF to form a stable complex [47,48]. The complex maintains the biological activity of bFGF [49] and can retard bFGF release from polymeric materials [50, 51]. Although covalently crosslinked, heparin-containing hydrogels have been shown to be useful for release of bFGF [52], physically cross-linked hydrogels could provide an alternative protein-delivery matrix without the need for potentially toxic crosslinking reagents.

The bFGF release and hydrogel erosion experiments were performed at 4 °C in 24-well polystyrene assay plates. A 2.5 wt.% solution of PEG-LMWH with bFGF was prepared via dissolving PEG-LMWH and bFGF in PBS at a final molar ratio of 1:1,500,000 (bFGF to LMWH). Secondly, a 5 wt.% solution of PEG-$PF4_{ZIP}$ in PBS was added to the PEG-LMWH/bFGF at a ligand molar ratio of 8:1 (LMWH:$PF4_{ZIP}$ dimer). Assuming that all $PF4_{ZIP}$ dimers bind LMWH, the molar ratio of bFGF to available LMWH in the PEG-LMWH/PEG-$PF4_{ZIP}$ hydrogel is 1:1,300,000. A 2.5 wt.% PEG-LMWH hydrogel was used as a control. The total amount of polymer in both samples was identical and bFGF was loaded at the same molar ratio for both the sample and the control.

Data from these release studies are summarized in Fig. 7. As shown in the figure, both gels show a burst release of approximately 25%, followed by a nearly linear slow release of bFGF over 10 days, to a maximum measured release of 35-40%. This initial release is similar to the initial burst release of some heparin-binding peptides from physically crosslinked, heparin-containing hydrogels [12]. The bFGF is released slightly more quickly from the PEG-LMWH controls than from the PEG-LMWH/PEG-$PF4_{ZIP}$ hydrogels, despite the slightly higher ratio of LMWH: bFGF in the control samples. The observed burst release is similar in value to previously reported burst release in other heparinized hydrogel systems [53]; the bFGF released from those hydrogel systems has been successfully applied to stimulate cell proliferation. Hydrogel erosion kinetics were also assessed for the samples used in release experiments. PEG-LMWH-Alexa Fluor 350 was pre-mixed with PEG-LMWH at a weight ratio of 1:158 to facilitate tracking of the eroded PEG-LMWH via fluorimetry. Fig. 8 presents hydrogel erosion data obtained for the PEG-LWMH/PEG-$PF4_{ZIP}$ hydrogel and the PEG-LMWH control. A burst erosion of 30%, followed by a slow erosion of both gels to a maximum of 40-50% erosion is indicated in this figure. These data also show that the erosion of the PEG-LMWH hydrogel

is faster than that of the PEG-LMWH /PEG-$PF4_{ZIP}$ hydrogel, which is in agreement with the bFGF release kinetics shown in Fig. 7.

Fig. 9 illustrates the comparison between the percentage of bFGF release at 8 days (near the end of the released experiments), the percentage of hydrogel erosion at 8 days and the storage modulus, $G'(\omega=0.1$ rad/s) (normalized by the storage modulus of PEG-LMWH) for various hydrogels. (Complete sets of bFGF release and hydrogel erosion data for the PEG-LMWH/PEG-HIP hydrogels are adapted from Ref. [12] and are compared to those of the PEG-LMWH/PEG-$PF4_{ZIP}$ hydrogels in Figs. A4 and A5.) It is shown in the figure that after 8 days, 40%, 36%, and 18% of bFGF are released from the PEG-LWMH control, the PEG-LWMH/PEG-$PF4_{ZIP}$ hydrogel, and the PEG-LWMH/PEG-HIP hydrogel, respectively. At the same time, 54% of the PEG-LWMH control, 45% of the PEG-LWMH/PEG-$PF4_{ZIP}$ hydrogel, and 22% of the PEG-LWMH/PEG-HIP hydrogel are eroded, indicating that release is directly correlated to hydrogel erosion. In addition, the normalized storage moduli are 1.05, and 3.37 for the PEG-LWMH/PEG-$PF4_{ZIP}$ hydrogel and the PEG-LWMH/PEG-HIP hydrogel, respectively (Fig. 9), while the release percentages are 36% and 18%. The correlation of decreased rates of release and hydrogel erosion with an increase in elastic moduli is therefore also suggested from these data.

4. Discussion

The engineering of novel materials to achieve desired delivery profiles is garnering increased attention in biomaterials science. Biologically-derived polymers, such as polysaccharides (alginate, chitosan, agarose, hyaluronic acid, dextran) and proteins (fibrin, collagen, gelatin), present candidate systems for drug delivery, but it is often difficult to engineer the properties of the natural matrices. Synthetic degradable polymers, such as poly(glycolic acid), poly(lactic acid), poly(ethylene glycol) (PEG), poly(lactideco-glycolide), and poly(ε-caprolactone), also provide useful matrices for drug delivery [54-56]. Among them, poly (glycolic acid) and poly (lactic acid) have been applied very frequently, but they can form proinflammatory fragments as a result of the acidic byproducts of their degradation. Noncovalent systems, such as those based on protein-protein interactions between antibodies and antigens [30] as well as others [31-33,56,57], have been explored and offer opportunities for the application of injectable delivery systems with controlled properties. However, less attention has been given to the interaction between peptides and other molecules in hydrogel assembly. Therefore the development of a set of new assembly motifs based on such peptide-polysaccharide interactions may offer an expanded set of strategies for producing therapeutic matrices capable of controlled protein delivery.

Accordingly, we have combined the use of coiled-coil motifs with their consequent binding of heparin for noncovalent assembly of growth-factor-binding hydrogels. Specifically, the $PF4_{ZIP}$ peptide was synthesized and attached to the termini of vinyl-sulfone modified star PEG. The $PF4_{ZIP}$ peptide, a GCN4-based coiled-coil motif designed to mimic the lysine-rich heparin-binding region of PF4 [34,58], was employed in these studies, with ultimate goals of expanding the number and types of binding interactions employed in hydrogel assembly and to manipulate materials properties and delivery profiles. The use of $PF4_{ZIP}$ was motivated by the fact that platelet factor 4 (PF4) is perhaps the strongest heparin-binding protein known [59]. The fact that the $PF4_{ZIP}$ peptide also binds strongly to heparin was confirmed via affinity chromatography and SPR experiments. The use of a smaller peptide with potent heparin binding affinity may permit more facile synthesis of active bioconjugates and assembly of hydrogels, as previously demonstrated [10-12].

LMWH was also anchored at the termini of star PEG molecules to produce the other assembly partner. LMWH is applied in this work in order to minimize the number of reactive groups on

the heparin toward PEG termini and therefore minimize crosslinking reactions during PEG-LMWH preparation. Hydrogels were assembled via interactions between LMWH and $PF4_{ZIP}$. These noncovalently crosslinked hydrogels offer many opportunities to deliver protein drugs, for example, growth factors, as a variety of growth factors, from structurally and biologically diverse protein families, possess affinity for heparin *in vitro*. In addition, binding to heparin may stabilize growth factors within a local sphere of action by protecting them from both diffusional and degradative loss [60], and in some cases may enhance binding to cell surface receptors [61].

The rheological properties of the hydrogels, as presented earlier, show a baseline elastic response (PEG-LMWH only) which most likely originates from physical interactions between LMWH termini of the four-arm star PEG, as also observed in previously reported hydrogels [11]. Such association of LMWH in PBS has been confirmed via dynamic light scattering experiments (data not shown). It is also clear that the addition of PEG-$PF4_{ZIP}$ provides further crosslinking that results in a significant increase in the elastic moduli. These results indicate that at the concentrations and on the timescales of the rheology experiments, the $PF4_{ZIP}$ adopts the coiled-coil structure capable of binding heparin (confirmed via CD and SPR experiments), and the $PF4_{ZIP}$ coiled-coils associate with LMWH to act as crosslinks. The bulk mechanical properties of this transient network are determined by relaxations that occur when the crosslinks are dissociated. SPR assessment of the dissociation rate constants of the $PF4_{ZIP}$-LMWH interaction indicates K_d values on the order of 10^{-3} s^{-1}, and the observation of a storage modulus that exceeds the loss modulus in the measured frequency regime is consistent with previous reports of other transiently crosslinked networks with crosslinks of similar off rates [62].

Although $PF4_{ZIP}$ shows a similar dissociation rate from heparin as those observed for the heparin-binding domains of ATIII and HIP (indicated via SPR experiments), PEG-$PF4_{ZIP}$ -based hydrogels exhibit lower normalized moduli at moderate to high HBP:LMWH ratios than hydrogels assembled via interactions between LMWH and other HBPs (Fig. 4). This likely results from the fewer number of binding sites for $PF4_{ZIP}$ on LMWH. Assuming that the frequency dependence of dynamic moduli (G' and G'') follow the Maxwell model, this result is consistent with the fact that fewer crosslinking points lead to lower dynamic moduli at low frequencies. These results therefore demonstrate that not only the kinetics of the LMWH-HBP interaction, but also the binding capacity of the LMWH for a given HBP, play important roles in determining rheological properties in these hydrogels. The moduli obtained in these and our previously reported hydrogel systems at 2.5 wt.% (100-200 Pa) are of useful range for soft tissue engineering applications, and could be increased via the use of more concentrated polymer solutions.

Identical moduli are obtained for the PEG-LMWH/PEG-$PF4_{ZIP}$ hydrogels from frequency sweep rheological measurements at 25 °C and 37 °C. This identical behavior is expected on the basis of our SPR investigations that indicate that the off-rate of the crosslinks does not vary significantly over this temperature range. Any contribution of changes in crosslink dissociation or density with temperature are therefore expected to be insignificant under these experimental conditions, leading to insignificant changes in rheological properties. From a practical perspective, these results indicate that the hydrogels exhibit sufficient elastic properties for application under physiological conditions [63-65]. The higher measured G' values in these PEG-$PF4_{ZIP}$-based hydrogels versus those previously reported arises in part from the higher modulus of the PEG-LMWH in these studies, which is likely a result of variations in the LMWH versus other preparation, which alter the extent of LMWH association.

In addition to their useful rheological properties at physiologically relevant temperatures, the shear recovery data in Fig. 6 also indicate the ability of these networks to recover from shear deformation. The differences in the rates of shear recovery observed for different hydrogels,

which ranged from immediate recovery for the hydrogels of Fig. 3 to gradual recovery for the hydrogels of Fig. 6, may be attributed to the multicomponent nature of the cross-linking in these systems, as both LMWH-LMWH and $PF4_{ZIP}$-LMWH interactions determine the rheological character of the gels. The resistance to flow in hydrogels is determined by the slower crosslinkers [66], and in SPR experiments. In SPR experiments, the LMWH-LMWH interactions are suggested to be much slower than $PF4_{ZIP}$-LMWH interactions (data not shown). When coupled with rheological data indicating base elastic behavior for the PEG-LMWH, these data confirm that LMWH-LMWH interactions dominate the rheological properties of the hydrogels. Given the heterogeneity in commercially available heparin preparations, variations in elastic modulus have been observed, and variations in the recovery of the hydrogels may therefore also be expected.

In addition to the rheological properties of these materials, the reported bFGF release rates from these hydrogels are also suggested to be useful, as they are comparable to those previously reported to be useful for neovascularization *in vivo* [50,67-69]. The increased rate of bFGF release relative to that observed for the previously reported PEG-LWMH/PEG-HIP hydrogel [11] is directly related to variations in the mechanical properties between these two classes of noncovalently assembled hydrogels and demonstrates the versatility of these compositions for mediating growth factor release. That the rates of bFGF release are also closely correlated with the rate of hydrogel erosion in all of these hydrogels suggests that bFGF may be released from the hydrogels while bound to the PEG-LMWH, which may improve the therapeutic efficacy of the protein. It has been shown in cell proliferation assays that bFGF delivered from covalently cross-linked PEG-LMWH hydrogels is bioactive (unpublished data), and the bioactivity of bFGF released from noncovalently crosslinked PEG-LWMH/PEG-$PF4_{ZIP}$ is under investigation. Taken altogether, the results of these and our previous investigations demonstrate that a range of erosion and release rates can be obtained for these noncovalently assembled systems, and that the rates of bFGF release can be modulated via choice of HBP or control of the mechanical properties of the hydrogels.

5. Conclusions

The $PF4_{ZIP}$ peptide was successfully employed for the non-covalent assembly of heparinized hydrogels. Multifunctional star PEG-$PF4_{ZIP}$ bioconjugates complexed with star PEG-LMWH form hydrogels that exhibit increasing elastic moduli with increasing mole ratio of PEG-$PF4_{ZIP}$. The viscoelastic properties of the hydrogels can be controlled via alterations in the ratio between LMWH and $PF4_{ZIP}$ peptide, and comparisons with other PEG-LMWH/PEG-HBP hydrogels suggests the importance of both LMWH/HBP binding kinetics and the binding capacity of LMWH in determining rheological properties in these hydrogels. Characterization of the PEG-LMWH/PEG-$PF4_{ZIP}$ hydrogels indicates that useful moduli for soft tissue engineering applications are obtained for these systems at physiological temperatures and after high shear, and these properties are consistent of those expected for a Maxwell fluid with crosslinks of the determined off rates. Further indication of the potential use of these systems in biological applications is offered by the bFGF release assays. The combination of bFGF release profiles and hydrogel erosion profiles suggests that bFGF delivery from the assembled hydrogels is mainly an erosion-controlled process that may permit co-release of bFGF with PEG-LMWH and may therefore also improve the bioactivity of bFGF delivered from these matrices. The use of a variety of HBPs permits control of the mechanical properties of the hydrogels, and therefore the rates of bFGF release can also be modulated. These results should also be generally applicable to other heparin-binding proteins. Hydrogels with such engineered mechanical properties and biological activities may find expanded use in controlled delivery of therapeutics and in other biological applications.

Acknowledgments

This research has been supported in part by grants from the National Institutes of Health (5 P20 RR15588; 1 R01 EB003172 01), the Arnold and Mabel Beckman Foundation, the University of Delaware Research Foundation, and the US Department of Defense (ARO). We thank Dr. Norman Wagner in the Department of Chemical Engineering (University of Delaware) for the use of the Paar Physica Rheometer and Dr. Mary Galvin in the Department of Materials Science and Engineering (University of Delaware) for the use of the FluoroMax-3 spectrofluorometer. Dr. Nori Yamaguchi is thanked for the many helpful suggestions and discussions.

Appendix A. The fitting method of concentration dependence of Δθ applied in CD

In the $PF4_{ZIP}$, the monomer-dimer transition follows a two-state equilibrium,

$$2M \leftrightarrow D \tag{A1}$$

The equilibrium constant of unfolding, K_d is defined as

$$K_d=[M]^2/[D]=2[M_0]f_m^2/(1-f_m) \tag{A2}$$

where $[M_0]$ is the total peptide concentration and f_m the fraction of the peptide in the monomeric form. f_m is followed by the change in the mean residue ellipticity at 222 nm, Δθ as a function of peptide concentration by

$$f_m=1-\Delta\theta/\Delta\theta_{max} \tag{A3}$$

$\Delta\theta = \theta - \theta_0$, where θ is the measured ellipticity and θ_0 is the ellipticity of the unfolded monomer, which was taken to be 2500 deg cm^2 $dmol^{-1}$ [67]. $\Delta\theta = \theta_{max} - \theta_0$, where θ_{max} is the ellipticity of the folded dimer. Following Eqs. (A2) and (A3), the dissociation constant K_d can be calculated from the following equation [68]:

$$K_d=[M]^2/[D]=2[M_0](1-\Delta\theta/\Delta\theta_{max})^2/(\Delta\theta/\Delta\theta_{max}) \tag{A4}$$

References

[1]. Johnson Z, Kosco-Vilbois MH, Herren S, Cirillo R, Muzio V, Zaratin P, Carbonatto M, Mack M, Smailbegovic A, Rose M, Lever R, Page C, Wells TNC, A.E.I. Proudfoot. Interference with heparin binding and oligomerization creates a novel anti-inflammatory strategy targeting the chemokine system. J. Immunol 2004;173(9):5776–5785. [PubMed: 15494530]

[2]. Coombe DR, Kett WC. Heparan sulfate-protein interactions: therapeutic potential through structure-function insights. Cell. Mol. Life Sci 2005;62(4):410–424. [PubMed: 15719168]

[3]. Capila I, Linhardt RJ. Heparin-protein interactions. Angew. Chem., Int. Ed. Engl 2002;41(3):391–412. [PubMed: 12491369]

[4]. Sasisekharan R, Venkataraman G. Heparin and heparan sulfate: biosynthesis, structure and function. Curr. Opin. Chem. Biol 2000;4(6):626–631. [PubMed: 11102866]

[5]. Mulloy B, Forster MJ, Jones C, Drake AF, Johnson EA, Davies DB. The effect of variation of substitution on the solution conformation of heparin — a spectroscopic and molecular modeling study. Carbohydr. Res 1994;255:1–26. [PubMed: 8181000]

[6]. Spillmann D, Lindahl U. Glycosaminoglycan protein interactions — a question of specificity. Curr. Opin. Struct. Biol 1994;4(5):677–682.

[7]. Fromm JR, Hileman RE, Caldwell EEO, Weiler JM, Linhardt RJ. Pattern and spacing of basic amino acids in heparin binding sites. Arch. Biochem. Biophys 1997;343(1):92–100. [PubMed: 9210650]

[8]. Kamei K, Wu XF, Xu XY, Minami K, Huy NT, Takano R, Kato H, Hara S. The analysis of heparin-protein interactions using evanescent wave biosensor with regioselectively desulfated heparins as the ligands. Anal. Biochem 2001;295(2):203–213. [PubMed: 11488623]

[9]. Fromm JR, Hileman RE, Weiler JM, Linhardt RJ. Interaction of fibroblast growth factor-1 and related peptides with heparan sulfate and its oligosaccharides. Arch. Biochem. Biophys 1997;346(2):252–262. [PubMed: 9343372]

[10]. Yamaguchi N, Kiick KL. Polysaccharide-poly(ethylene glycol) star copolymers as scaffolds for the production of bioactive hydrogels. Biomacromolecules 2005;6(4):1921–1930. [PubMed: 16004429]

[11]. Yamaguchi N, Chae BS, Zhang L, Kiick KL, Furst EM. Rheological characterization of polysaccharide-poly(ethylene glycol) star copolymer hydrogels. Biomacromolecules 2005;6(4): 1931–1940. [PubMed: 16004430]

[12]. Seal BL, Panitch A. Physical polymer matrices based on affinity interactions between peptides and polysaccharides. Biomacromolecules 2003;4(6):1572–1582. [PubMed: 14606882]

[13]. Peppas NA, Wood KM, Blanchette JO. Hydrogels for oral delivery of therapeutic proteins. Expert Opin. Biol. Ther 2004;4(6):881–887. [PubMed: 15174970]

[14]. Zalipsky S. Functionalized poly(ethylene glycol) for preparation of biologically relevant conjugates. Bioconjug. Chem 1995;6(2):150–165. [PubMed: 7599259]

[15]. Zisch AH, Lutolf MP, Hubbell JA. Biopolymeric delivery matrices for angiogenic growth factors. Cardiovasc. Pathol 2003;12(6):295–310. [PubMed: 14630296]

[16]. Nivasu VM, Yarapathi RV, Tammishetti S. Synthesis, UV photo-polymerization and degradation study of PEG containing polyester polyol acrylates. Polym. Adv. Technol 2004;15(3):128–133.

[17]. Zheng YJ, Mieie M, Mello SV, Mabrouki M, Andreopoulos FM, Konka V, Pham SM, Leblanc RM. PEG-based hydrogel synthesis via the photodimerization of anthracene groups. Macromolecules 2002;35(13):5228–5234.

[18]. Brown CD, Stayton PS, Hoffman AS. Semi-interpenetrating network of poly(ethylene glycol) and poly(D,L-lactide) for the controlled delivery of protein drugs. J. Biomater. Sci., Polym. Ed 2005;16 (2):189–201. [PubMed: 15794485]

[19]. Cellesi F, Tirelli N, Hubbell JA. Materials for cell encapsulation via a new tandem approach combining reverse thermal gelation and covalent crosslinking. Macromol. Chem. Phys 2002;203 (1011):1466–1472.

[20]. Lutolf MP, Tirelli N, Cerritelli S, Cavalli L, Hubbell JA. Systematic modulation of Michael-type reactivity of thiols through the use of charged amino acids. Bioconjug. Chem 2001;12(6):1051–1056. [PubMed: 11716699]

[21]. Moffat KL, Marra KG. Biodegradable poly(ethylene glycol) hydrogels crosslinked with genipin for tissue engineering applications. J. Biomed. Mater. Res. Part B 2004;71B(1):181–187.

[22]. Lutolf MR, Weber FE, Schmoekel HG, Schense JC, Kohler T, Muller R, Hubbell JA. Repair of bone defects using synthetic mimetics of collagenous extracellular matrices. Nat. Biotechnol 2003;21(5):513–518. [PubMed: 12704396]

[23]. Taylor SJ, McDonald JW, Sakiyama-Elbert SE. Controlled release of neurotrophin-3 from fibrin gels for spinal cord injury. J. Control. Release 2004;98(2):281–294. [PubMed: 15262419]

[24]. Bourke SL, Al-Khalili M, Briggs T, Michniak BB, Kohn J, Poole-Warren LA. A photo-crosslinked poly(vinyl alcohol) hydrogel growth factor release vehicle for wound healing applications. AAPS Pharmsci 2003;5(4)

[25]. Seliktar D, Zisch AH, Lutolf MP, Wrana JL, Hubbell JA. MMP-2 sensitive, VEGF-bearing bioactive hydrogels for promotion of vascular healing. J. Biomed. Mater. Res. Part A 2004;68A(4):704–716.

[26]. Sakiyama-Elbert S, Hubbell J. Functional biomaterials: design of novel biomaterials. Ann. Rev. Mater. Res 2001;31:183–201.

[27]. Sakiyama-Elbert SE, Hubbell JA. Development of fibrin derivatives for controlled release of heparin-binding growth factors. J. Control. Release 2000;65(3):389–402. [PubMed: 10699297]

[28]. Sakiyama-Elbert SE, Hubbell JA. Controlled release of nerve growth factor from a heparin-containing fibrin-based cell ingrowth matrix. J. Control. Release 2000;69(1):149–158. [PubMed: 11018553]

[29]. Hennink WE, van Nostrum CF. Novel crosslinking methods to design hydrogels. Adv. Drug Deliv. Rev 2002;54(1):13–36. [PubMed: 11755704]

[30]. Miyata T, Asami N, Uragami T. A reversibly antigen-responsive hydrogel. Nature 1999;399(6738): 766–769. [PubMed: 10391240]

[31]. Xu CY, Breedveld V, Kopecek J. Reversible hydrogels from self-assembling genetically engineered protein block copolymers. Biomacro-molecules 2005;6(3):1739–1749.

[32]. Wang C, Stewart RJ, Kopecek J. Hybrid hydrogels assembled from synthetic polymers and coiled-coil protein domains. Nature 1999;397(6718):417–420. [PubMed: 9989405]

[33]. Petka WA, Harden JL, McGrath KP, Wirtz D, Tirrell DA. Reversible hydrogels from self-assembling artificial proteins. Science 1998;281(5375):389–392. [PubMed: 9665877]

[34]. Butcher DJ, Kowalska MA, Li S, Luo ZW, Shan SM, Lu ZX, Niewiarowski S, Huang ZW. A natural motif approach to protein design: a synthetic leucine zipper peptide mimics the biological function of the platelet factor 4 protein. FEBS Lett 1997;409(2):183–187. [PubMed: 9202142]

[35]. Casper CL, Yamaguchi N, Kiick KL, Rabolt JF. Functionalizing electrospun fibers with biologically relevant macromolecules. Biomacro-molecules 2005;6(4):1998–2007.

[36]. Zitzewitz JA, Bilsel O, Luo JB, Jones BE, Matthews CR. Probing the folding mechanism of a leucine-zipper peptide by stopped-flow circular-dichroism spectroscopy. Biochemistry 1995;34 (39):12812–12819. [PubMed: 7548036]

[37]. Zitzewitz JA, Ibarra-Molero B, Fishel DR, Terry KL, Matthews CR. Preformed secondary structure drives the association reaction of GCN4-p1, a model coiled-coil system. J. Mol. Biol 2000;296(4): 1105–1116. [PubMed: 10686107]

[38]. Sosnick TR, Jackson S, Wilk RR, Englander SW, DeGrado WF. The role of helix formation in the folding of a fully alpha-helical coiled coil. Proteins 1996;24(4):427–432. [PubMed: 9162943]

[39]. Moran LB, Schneider JP, Kentsis A, Reddy GA, Sosnick TR. Transition state heterogeneity in GCN4 coiled coil folding studied by using multisite mutations and crosslinking. Proc. Natl. Acad. Sci. U. S. A 1999;96(19):10699–10704. [PubMed: 10485889]

[40]. Holtzer ME, Bretthorst GL, d'Avignon DA, Angeletti RH, Mints L, Holtzer A. Temperature dependence of the folding and unfolding kinetics of the GCN4 leucine zipper via C-13(alpha)-NMR. Biophys. J 2001;80(2):939–951. [PubMed: 11159461]

[41]. d'Avignon DA, Bretthorst GL, Holtzer ME, Holtzer A. Thermodynamics and kinetics of a folded-folded ' transition at valine-9 of a GCN4-like leucine zipper. Biophys. J 1999;76(5):2752–2759. [PubMed: 10233090]

[42]. Ibarra-Molero B, Zitzewitz JA, Matthews CR. Salt-bridges can stabilize but do not accelerate the folding of the homodimeric coiled-coil peptide GCN4-p1. J. Mol. Biol 2004;336(5):989–996. [PubMed: 15037063]

[43]. Knappenberger JA, Smith JE, Thorpe SH, Zitzewitz JA, Matthews CR. A buried polar residue in the hydrophobic interface of the coiled-coil peptide, GCN4-p1, plays a thermodynamic, not a kinetic role in folding. J. Mol. Biol 2002;321(1):1–6. [PubMed: 12139928]

[44]. Gosal WS, Clark AH, Pudney PDA, Ross-Murphy SB. Novel amyloid fibrillar networks derived from a globular protein: beta-lactoglobulin. Langmuir 2002;18(19):7174–7181.

[45]. Ibel K, Poland GA, Baldwin JP, Pepper DS, Luscombe M, Holbrook JJ. Low-resolution structure of the complex of human blood platelet factor 4 with heparin determined by small-angle neutron scattering. Biochim. Biophys. Acta 1986;870(1):58–63. [PubMed: 3947648]

[46]. Liu SC, Zhou FY, Hook M, Carson DD. A heparin-binding synthetic peptide of heparin/heparan sulfate-interacting protein modulates blood coagulation activities. Proc. Natl. Acad. Sci. U. S. A 1997;94(5):1739–1744. [PubMed: 9050848]

[47]. DiGabriele AD, Lax I, Chen DI, Svahn CM, Jaye M, Schlessinger J, Hendrickson WA. Structure of a heparin-linked biologically active dimer of fibroblast growth factor. Nature 1998;393(6687): 812–817. [PubMed: 9655399]

[48]. Faham S, Hileman RE, Fromm JR, Linhardt RJ, Rees DC. Heparin structure and interactions with basic fibroblast growth factor. Science 1996;271(5252):1116–1120. [PubMed: 8599088]

[49]. Yayon A, Klagsbrun M, Esko JD, Leder P, Ornitz DM. Cell-surface, heparin-like molecules are required for binding of basic fibroblast growth-factor to its high-affinity receptor. Cell 1991;64(4): 841–848. [PubMed: 1847668]

[50]. Jeon O, Ryu SH, Chung JH, Kim BS. Control of basic fibroblast growth factor release from fibrin gel with heparin and concentrations of fibrinogen and thrombin. J. Control. Release 2005;105(3): 249–259. [PubMed: 16088988]

[51]. Ohta M, Suzuki Y, Chou H, Ishikawa N, Suzuki S, Tanihara M, Mizushima Y, Dezawa M, Ide C. Novel heparin/alginate gel combined with basic fibroblast growth factor promotes nerve regeneration in rat sciatic nerve. J. Biomed. Mater. Res. Part A 2004;71A(4):661–668.

[52]. Cai SS, Liu YC, Shu XZ, Prestwich GD. Injectable glycosaminoglycan hydrogels for controlled release of human basic fibroblast growth factor. Biomaterials 2005;26(30):6054–6067. [PubMed: 15958243]

[53]. Wissink MJB, Beernink R, Pieper JS, Poot AA, Engbers GHM, Beugeling T, van Aken WG, Feijen J. Binding and release of basic fibroblast growth factor from heparinized collagen matrices. Biomaterials 2001;22(16):2291–2299. [PubMed: 11456069]

[54]. Langer R, Peppas NA. Advances in biomaterials, drug delivery, and bionanotechnology. Aiche J 2003;49(12):2990–3006.

[55]. Moses MA, Brem H, Langer R. Advancing the field of drug delivery: taking aim at cancer. Cancer Cell 2003;4(5):337–341. [PubMed: 14667500]

[56]. Seal BL, Otero TC, Panitch A. Polymeric biomaterials for tissue and organ regeneration. Mater. Sci. Eng., R Rep 2001;34(45):147–230.

[57]. Wright ER, Conticello VP. Self-assembly of block copolymers derived from elastin-mimetic polypeptide sequences. Adv. Drug Deliv. Rev 2002;54(8):1057–1073. [PubMed: 12384307]

[58]. Deuel TF, Keim PS, Farmer M, Heinrikson RL. Amino-acid sequence of human platelet factor 4. Proc. Natl. Acad. Sci. U. S. A 1977;74(6):2256–2258. [PubMed: 267922]

[59]. Zhang XH, Chen LQ, Bancroft DP, Lai CK, Maione TE. Crystal-structure of recombinant human platelet factor-4. Biochemistry 1994;33(27):8361–8366. [PubMed: 8031770]

[60]. McCaffrey TA, Falcone DJ, Vicente D, Du BH, Consigli S, Borth W. Protection of transforming growth-factor-beta-1 activity by heparin and fucoidan. J. Cell. Physiol 1994;159(1):51–59. [PubMed: 7511146]

[61]. Roghani M, Mansukhani A, Dellera P, Bellosta P, Basilico C, Rifkin DB, Moscatelli D. Heparin increases the affinity of basic fibroblast growth-factor for its receptor but is not required for binding. J. Biol. Chem 1994;269(6):3976–3984. [PubMed: 8307953]

[62]. Yount WC, Loveless DM, Craig SL. Small-molecule dynamics and mechanisms underlying the macroscopic mechanical properties of coordinatively cross-linked polymer networks. J. Am. Chem. Soc 2005;127(41):14488–14496. [PubMed: 16218645]

[63]. Lindblad MS, Albertsson AC, Ranucci E, Laus M, Giani E. Biodegradable polymers from renewable sources: rheological characterization of hemicellulose-based hydrogels. Biomacromolecules 2005;6(2):684–690. [PubMed: 15762630]

[64]. Broderick EP, O'Halloran DM, Rochev YA, Griffin M, Collighan RJ, Pandit AS. Enzymatic stabilization of gelatin-based scaffolds. J. Biomed. Mater. Res. Part B 2005;72B(1):37–42.

[65]. Dalton PD, Flynn L, Shoichet MS. Manufacture of poly(2-hydroxyethyl methacrylate-co-methyl methacrylate) hydrogel tubes for use as nerve guidance channels. Biomaterials 2002;23(18):3843–3851. [PubMed: 12164188]

[66]. Loveless DM, Jeon SL, Craig SL. Rational control of viscoelastic properties in multicomponent associative polymer networks. Macromolecules 2005;38(24):10171–10177.

[67]. Chinen N, Tanihara M, Nakagawa M, Shinozaki K, Yamamoto E, Mizushima Y, Suzuki Y. Action of microparticles of heparin and alginate crosslinked gel when used as injectable artificial matrices to stabilize basic fibroblast growth factor and induce angiogenesis by controlling its release. J. Biomed. Mater. Res. Part A 2003;67A(1):61–68.

[68]. Ishihara M, Obara K, Ishizuka T, Fujita M, Sato M, Masuoka K, Saito Y, Yura H, Matsui T, Hattori H, Kikuchi M, Kurita A. Controlled release of fibroblast growth factors and heparin from photocrosslinked chitosan hydrogels and subsequent effect on *in vivo* vascularization. J. Biomed. Mater. Res. Part A 2003;64A(3):551–559.

[69]. Wissink MJB, Beernink R, Poot AA, Engbers GHM, Beugeling T, van Aken WG, Feijen J. Improved endothelialization of vascular grafts by local release of growth factor from heparinized collagen matrices. J. Control. Release 2000;64(13):103–114. [PubMed: 10640649]

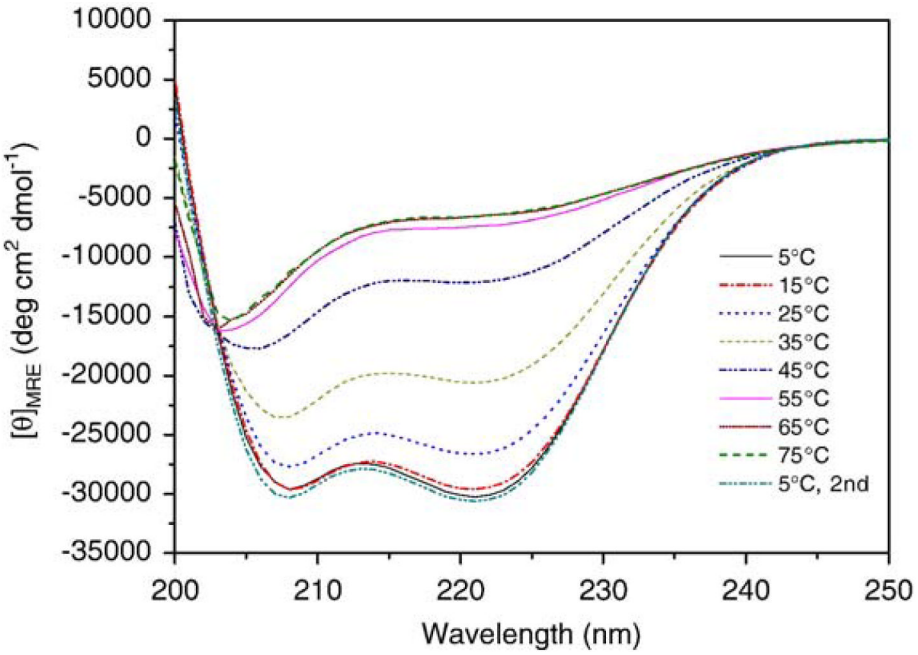

Fig. 1.

CD spectra of $PF4_{ZIP}$ at different temperatures, at a $PF4_{ZIP}$ concentration of 150 μM in PBS.

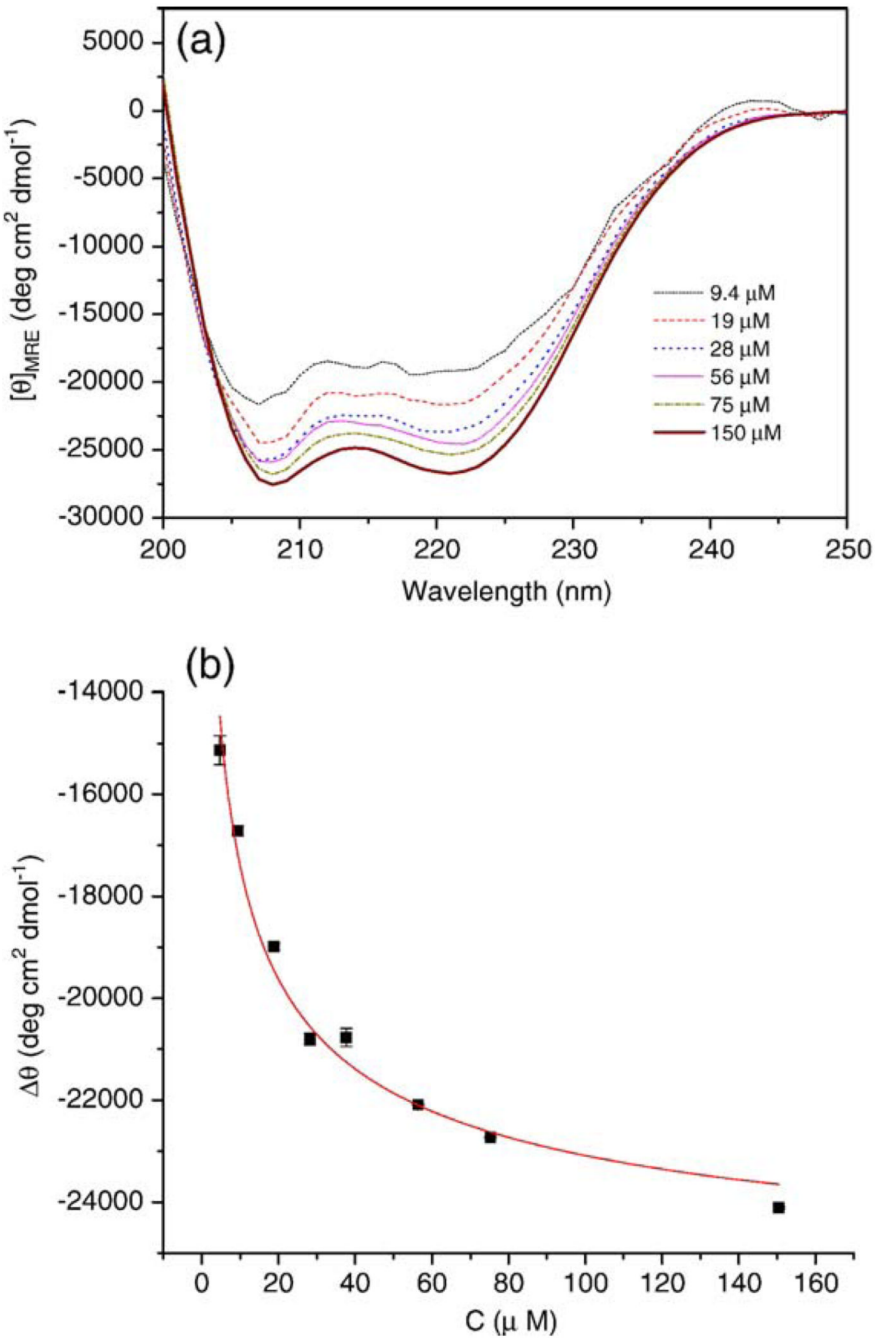

Fig. 2.

(a) CD spectra of $PF4_{ZIP}$ at different concentrations in PBS at 25 °C. (b) Concentration dependence of the MRE_{222} for $PF4_{ZIP}$. The solid line is the best fit according to Eq. (A4), with K_d=3.48±0.03 μM. θ_0 was fixed at 2500 deg cm^2dmol^{-1}. The errors are derived from the average of duplicate measurements on separate samples.

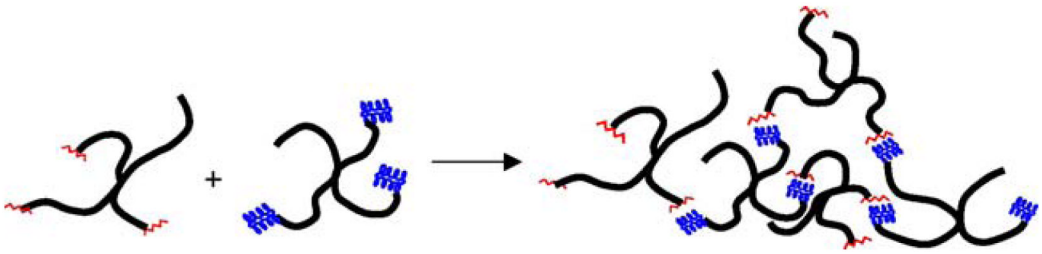

Scheme 1.

Schematic of the assembly of hydrogels from solutions of the two polymer conjugates. The $PF4_{ZIP}$ is rendered as an oligomerized coiled-coil, as its concentration (200 μM) under these experimental conditions is two orders of magnitude greater than the measured K_d value.

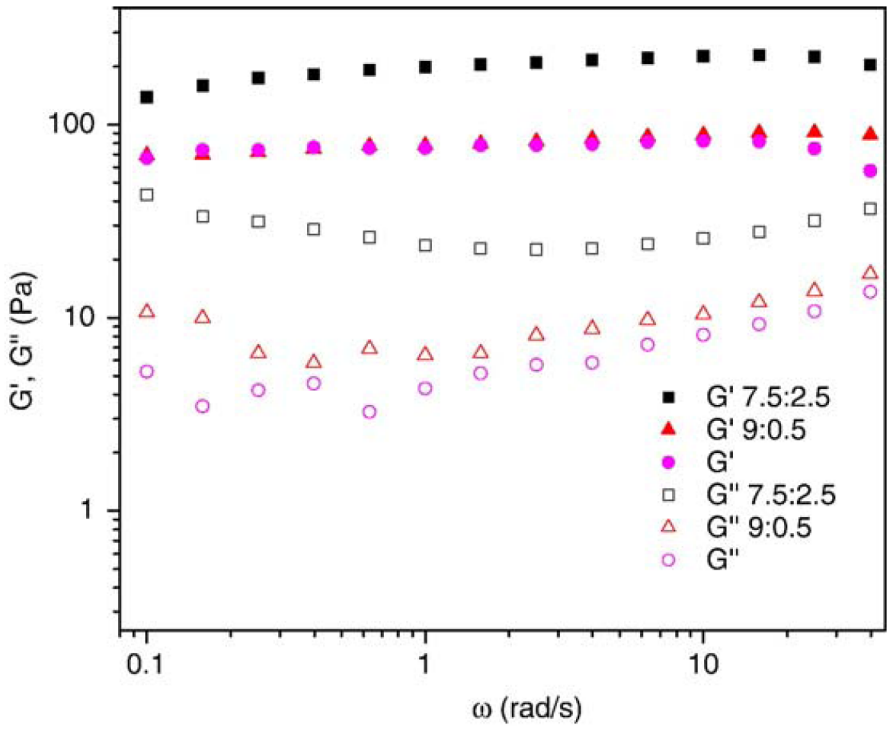

Fig. 3.

Storage moduli (closed symbols) and loss moduli (open symbols) of the PEG-LMWH/PEG-$PF4_{ZIP}$ hydrogels for varying molar ratios of LMWH:$PF4_{ZIP}$ (squares 7.5:2.5; triangles 9:0.5). The response of 2.5 wt.% of the PEG-LMWH (circles) is shown for comparison.

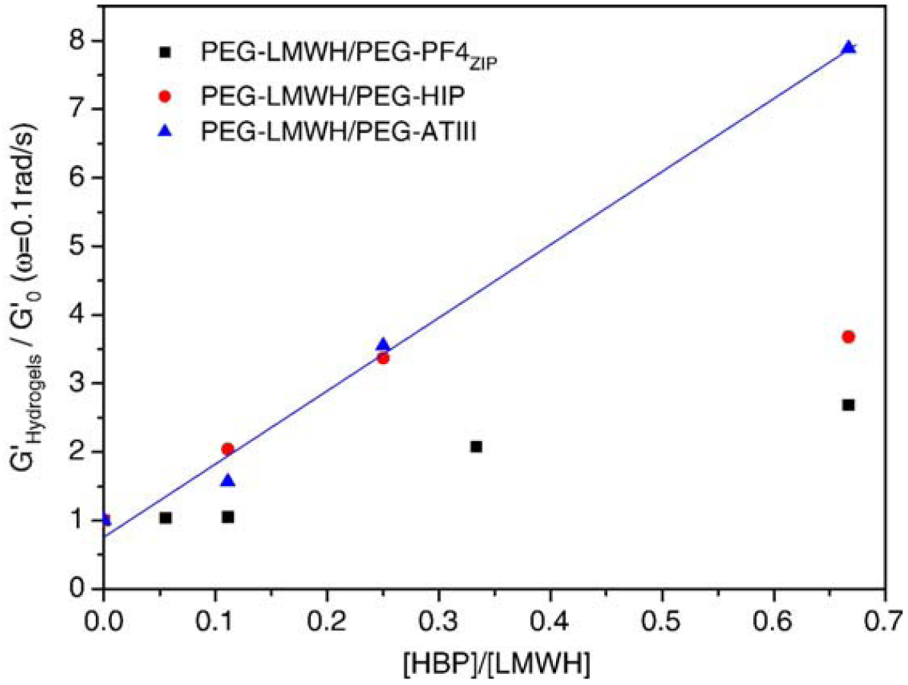

Fig. 4.

Plots of normalized storage moduli *G′* (ω=0.1 rad/s) as a function of HBP ($PF4_{ZIP}$ (squares), HIP (circles), or ATIII (triangles)) to LMWH. HIP and ATIII data are adapted from Ref. [11].

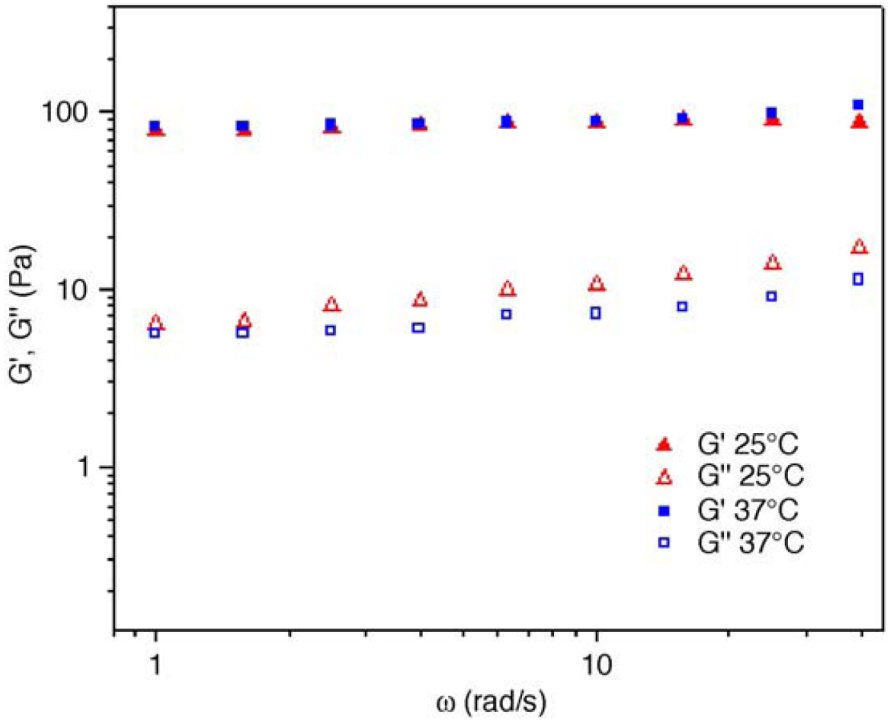

Fig. 5.

Comparison of storage moduli (closed symbols) and loss moduli (open symbols) of the PEG-LMWH/PEG-$PF4_{ZIP}$ hydrogels (LMWH:$PF4_{ZIP}$=9:0.5) obtained at 25 °C (triangles) and 37 °C (squares).

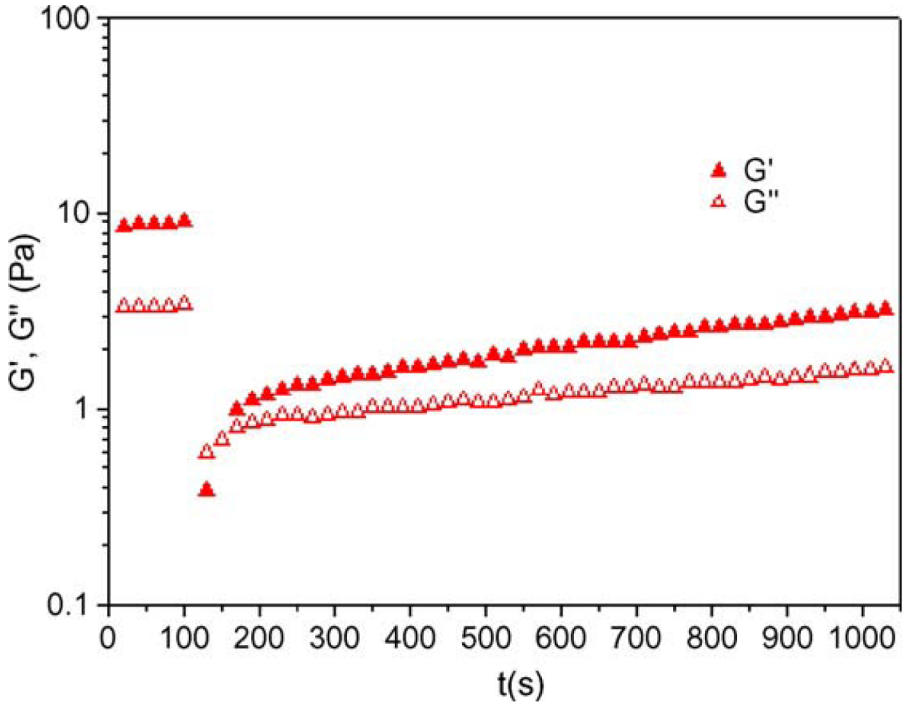

Fig. 6.
Shear recovery data for PEG-LMWH/PEG-$PF4_{ZIP}$ hydrogels (LMWH: $PF4_{ZIP}$=9:1; ω=10 rad/s) at 25 °C.

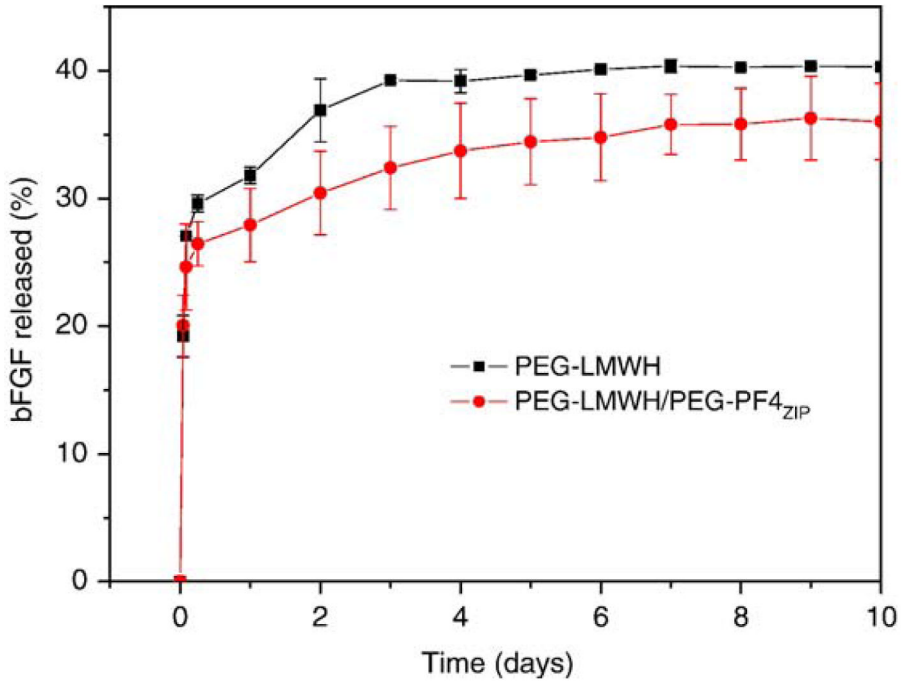

Fig. 7.

The bFGF release profiles of the PEG-LWMH/PEG-$PF4_{ZIP}$ hydrogel (LMWH:$PF4_{ZIP}$=8:1, circles) and the PEG-LMWH control (squares). The errors are derived from the average of duplicate measurements.

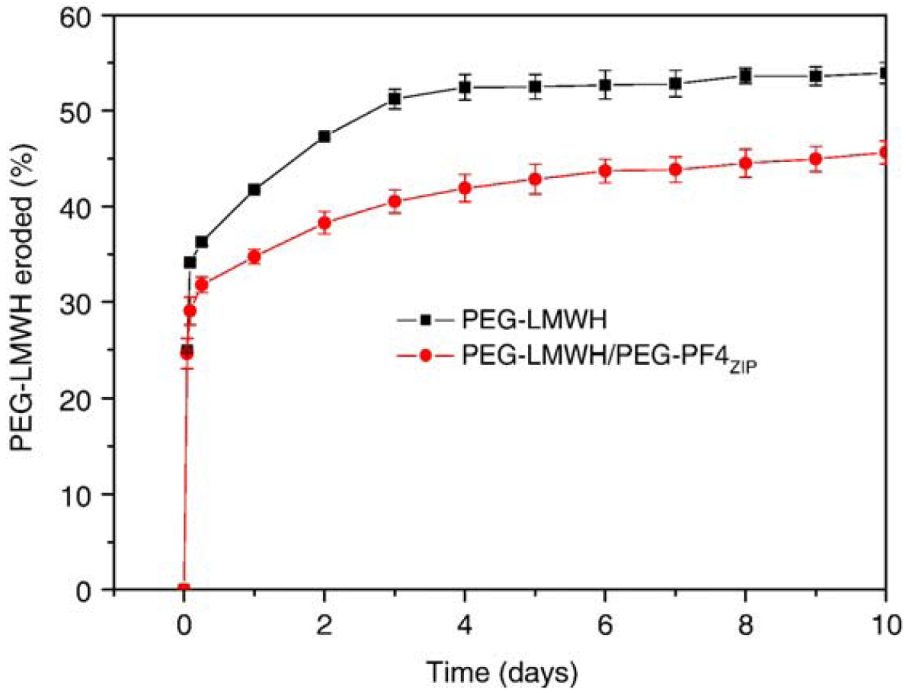

Fig. 8.

The erosion profiles of the PEG-LWMH/PEG-$PF4_{ZIP}$ hydrogel (LMWH:$PF4_{ZIP}$=8:1, circles) and the PEG-LMWH control (squares). The errors are derived from the average of duplicate measurements.

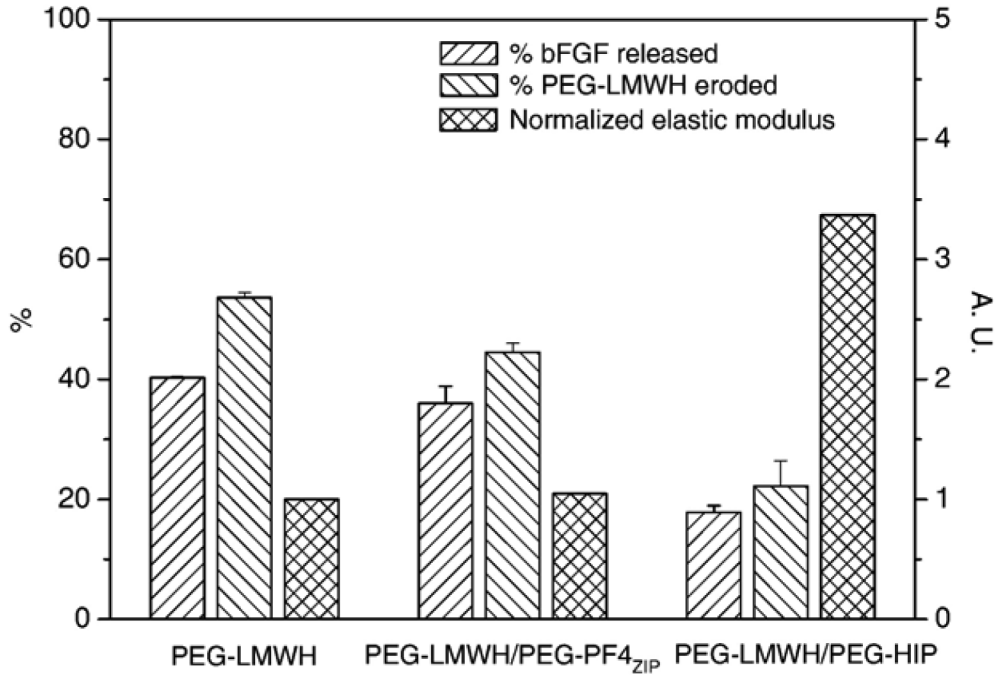

Fig. 9.

Comparison of the percentage of bFGF release after 8 days, the percentage of hydrogel erosion after 8 days and the storage modulus, $G'(\omega=0.1$ rad/s) (normalized by the storage modulus of the PEG-LMWH) for various hydrogels. The PEG-LWMH/PEG-HIP hydrogel (LMWH:HIP=8:2) data are adapted from Ref. [12]. The errors are derived from the average of duplicate measurements.

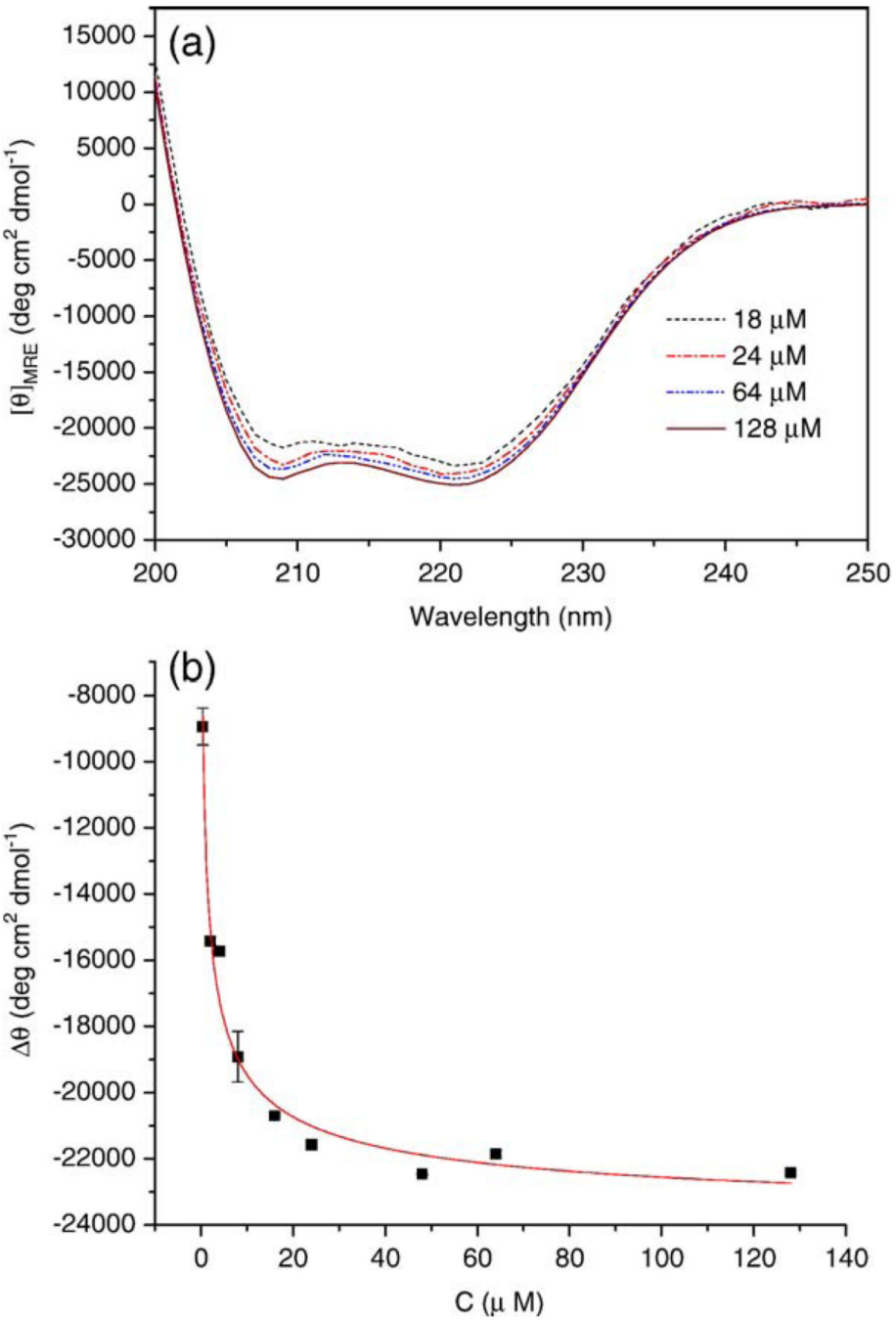

Fig. A1.

(a) CD spectra of PEG-PF4$_{ZIP}$ at different concentrations in PBS at 25 °C. (b) Concentration dependence of the MRE for PEG-PF4$_{ZIP}$ at 222 nm. The solid line is the best fit according to Eq. (A4) for $K_d = 0.93 \pm 0.01$ μM. θ_0 was fixed at 2500 deg cm^2 dmol^{-1}. The errors are derived from the average of duplicate measurements.

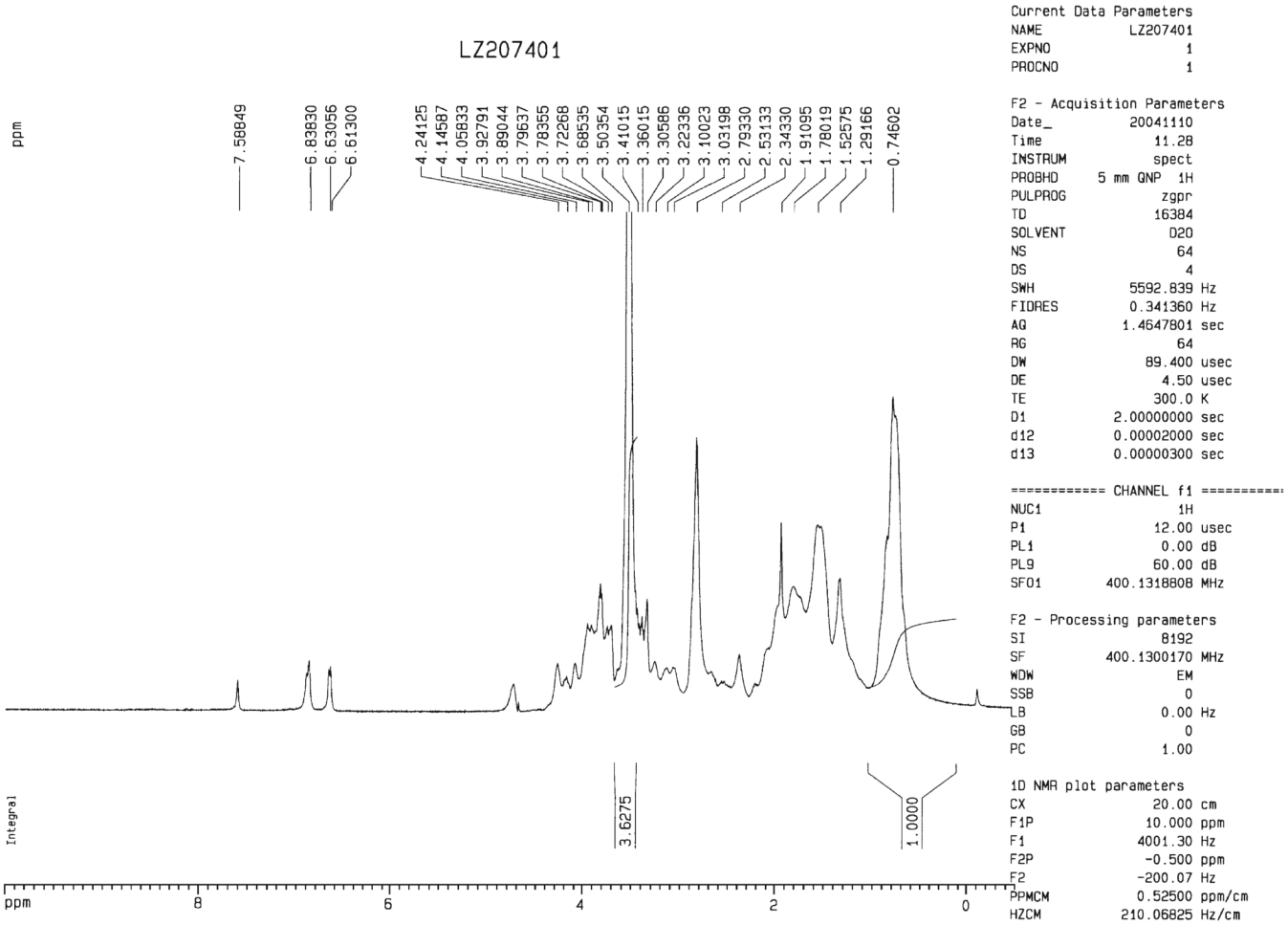

Fig. A2.

The ^{1}H NMR spectrum of the PEG-$PF4_{ZIP}$ recorded in D_2O. The PEG peak at 3.50 ppm was integrated against the δCH_3 from Leu and Val residues observed in the region between 0.2 to 1.0 ppm in spectra of the $PF4_{ZIP}$. Integration of $PF4_{ZIP}$ resonances in this region, and comparison with the PEG backbone resonance revealed an average functionalization of the star PEG with $PF4_{ZIP}$ dimer in PEG-$PF4_{ZIP}$ to be 59%, indicating that an average of 2.4 out of four-arms have been functionalized with $PF4_{ZIP}$ dimer.

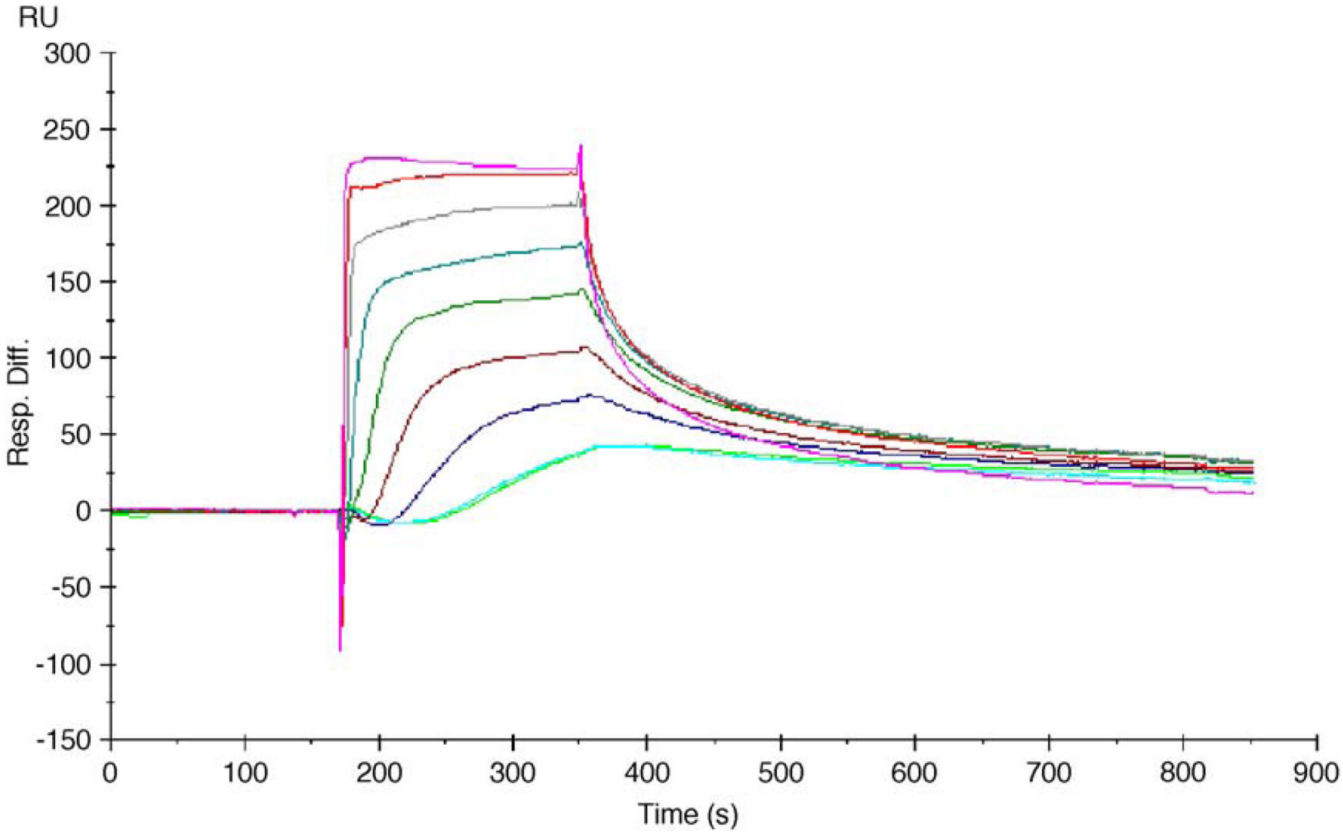

Fig. A3.
The sensorgrams for the interaction of $PF4_{ZIP}$ with the LMWH-modified chip surface. Concentration from top to bottom: 4096, 2048, 1024, 512, 256, 128, 64, 32 nM (repeated twice).

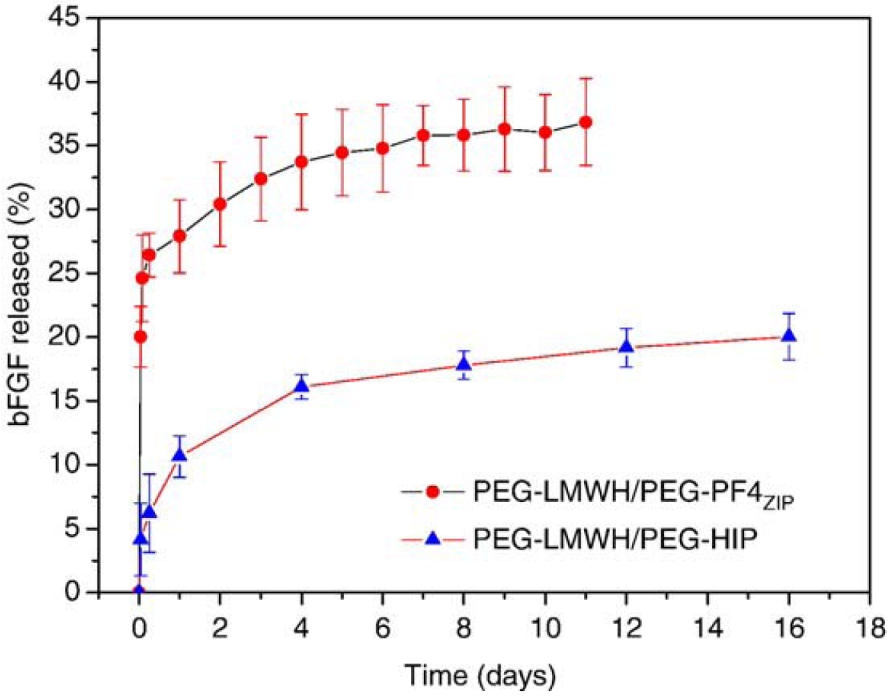

Fig. A4.

The bFGF release profiles of the PEG-LWMH/PEG-$PF4_{ZIP}$ hydrogel and the PEG-LWMH/PEG-HIP hydrogel. The errors are derived from the average of duplicate measurements.

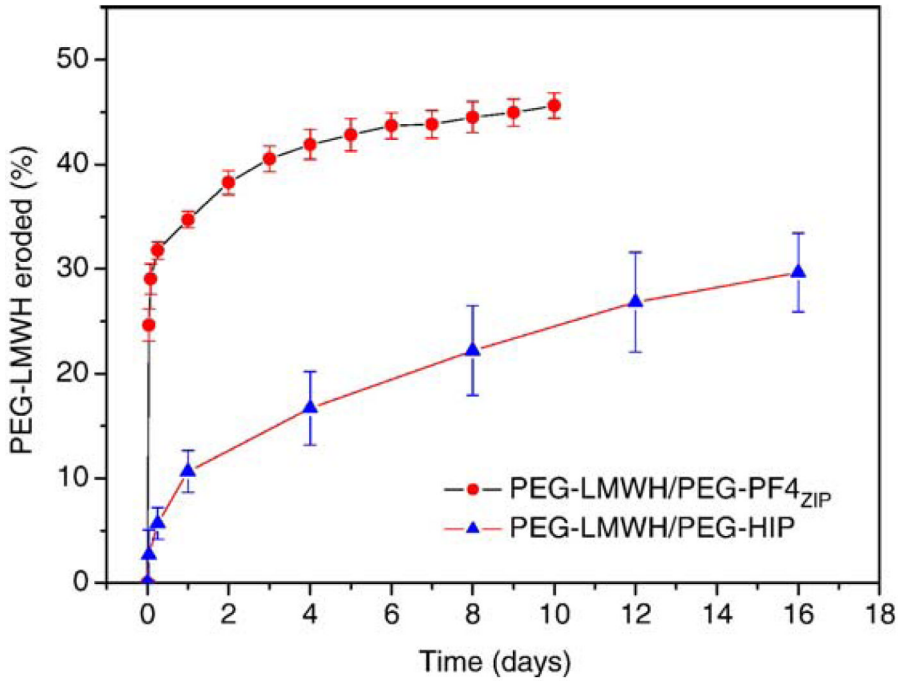

Fig. A5.

The erosion profiles of the PEG-LWMH/PEG-$PF4_{ZIP}$ hydrogel and the PEG-LWMH/PEG-HIP hydrogel. The errors are derived from the average of duplicate measurements.

Table 1

Heparin binding affinity data (at 25 °C) for heparin-binding peptides determined via affinity chromatography and SPR

Peptide	Salt required for elution from heparin column (mM)	k_a ($M^{-1}s^{-1}$)	k_d (s^{-1})	K_D (μM)
ATIII[a]	594±2	1.56± 0.06×10^2	2.00± 0.3×10^{-3}	12.9±1.3
HIP[a]	687±1	1.10± 0.08×10^3	4.64± 0.02×10^{-3}	4.20±0.3
$PF4_{ZIP}$	962±10	2.24± 0.05×10^5	2.56± 0.10×10^{-3}	1.15± 0.03×10^{-2}

The errors are derived from the average of duplicate measurements.

[a] Data from previously reported studies [12].

Table 2

Heparin-binding affinity data for $PF4_{ZIP}$ at different temperatures, as determined via SPR

Temperature (°C)	k_a ($M^{-1}s^{-1}$)	k_d (s^{-1})	K_D (μM)
5	$1.56\pm0.01\times10^{5}$	$3.74\pm0.17\times10^{-3}$	$2.41\pm0.10\times10^{-8}$
15	$1.90\pm0.04\times10^{5}$	$1.67\pm0.03\times10^{-3}$	$8.82\pm0.02\times10^{-9}$
25	$2.24\pm0.05\times10^{5}$	$2.56\pm0.10\times10^{-3}$	$1.15\pm0.03\times10^{-8}$
37	$5.11\pm0.02\times10^{5}$	$2.44\pm0.08\times10^{-3}$	$4.78\pm0.14\times10^{-9}$

The errors are derived from the average of duplicate measurements.